Online Maximum Torque per Flux for Direct Torque and Flux Control of IPMSM Drives

Soroush Ahooye Atashin
Dep. Of electrical engineering
Ferdowsi university of Mashad
Mashad, Iran
atasheen.soroush@mail.um.ac.ir

Hossein Abootorabi Zarchi
Dep. Of electrical engineering
Ferdowsi University of Mashad
Mashhad, Iran
abootorabi@um.ac.ir

Gholam Reza Arab Markade*h*
Dep. Of electrical engineering
University of Shahrekord
Shahrekord, Iran
arab-gh@eng.sku.ac.ir

***Abstract*—Interior permanent magnet synchronous machine (IPMSM) is capable of operating in field weakening region. In order to employ this feature, field weakening control should be considered in the control scheme. Furthermore, the IPMSM whose current characteristic is inside the current limit circle can operate above critical speed. This study presents a novel approach of achieving maximum torque per flux (MTPF) strategy for IPMSM to operate above critical speed. The MTPF equation is derived based on Lagrange's theorem and implemented by MTPF bloc in the proposed control scheme which is based on direct torque flux control (DTFC). The algorithm and scheme are simple and can operate continuously in the both constant torque and FW regions. Hence, the scheme can extend the speed operating of the machine. Besides, it can operate in all different operating conditions and achieve maximum torque. The simulation results confirm the stability of proposed scheme.**

Keywords—interior permanent magnet synchronous machine (IPMSM), direct torque flux control (DTFC), field weakening, maximum torque per flux (MTPF).

I. INTRODUCTION

Due to the absence of field circuit in interior permanent magnet synchronous machine (IPMSM), it has high efficiency, simple control, high reliability, less noise in comparison to the others [1]. Furthermore, it has a wide constant power suitable for electric vehicles and home appliances. General control schemes are either field-oriented control (FOC) or direct torque control (DTC) for IPMSM [2]. Since DTC renders a better response time, robust to parameters, it is preferred for high dynamic applications [3]. However, conventional DTC has a variable switching frequency so that torque ripple and noise are significant in high speed [4]. Hence, a modified DTC scheme or DTC based space vector modulation (SVM) have been proposed to decrease ripple in torque and current [5,6]. The DTC based SVM is so called direct torque flux control (DTFC). Nowadays, DTFC has received paramount attention among researchers owing to simplicity and fast response. As IPMSM is able to operate in the field weakening (FW) region, various control schemes have been introduced to operate in FW region based on the DTC scheme.

DTFC based on look-up tables (LUTs) has been recommended to operate in the constant torque (CT) and the FW regions [7,8]. In [7], proposed scheme was sensorless and able to operate in the maximum torque per voltage (MTPV) region. In [8], one variable coefficient was introduced to modify flux and then current references are produced based on inputs torque and flux. It is important to be noted that the LUT considered the parameter variations. In [9], although torque angle control was used to operate in MTPV region, production of flux is done by LUT. However, these schemes need laboratory tests to create LUT to operate in wide speed range. In [10,11], computational method has been introduced to generate flux of CT and FW regions. Moreover, MTPV strategy was employed without offline calculation in the proposed scheme. Novel approach of maximum torque per flux (MTPF) has been introduced based on DTFC scheme in [12,13]. In [12], the MTPF equation was achieved to generate optimum flux by using analytical method and approximation.

In this paper, a novel technique is introduced to operate IPMSM in MTPF trajectory. The proposed method can produce the required torque for MTPF region based on Lagrange's theorem. Also, the proposed scheme is based on DTFC and can operate in wide speed range for both motoring and generating operation.

This paper is organized as follows: section II describes the DTFC of IPMSM to operate in wide speed range. Section III explains the proposed MTPF and the equation is derived. Section IV presents the DTFC scheme and simulation results are discussed in section V. And finally, the conclusion is highlighted in section VI.

II. DIRECT TORQUE FLUX CONTROL BASED ON IPMSM

A. Mathematical Equations of IPMSM

Figure 1 shows the vector diagram which consist of the stationary, rotor and stator flux reference frames. The voltage and torque equations of IPMSM can be expressed in the rotor reference frame as:

$$v_d = R_s i_d + L_d \frac{di_d}{dt} - \omega_e L_q i_q \quad (1)$$

$$v_q = R_s i_q + L_q \frac{di_q}{dt} + \omega_e (L_d i_d + \lambda_m) \quad (2)$$

$$T_e = \frac{3p}{2}\left(\lambda_m i_q + (L_d - L_q) i_d i_q\right) \quad (3)$$

where R_s, ω_e and p are the stator resistance, electrical speed and number of pole pairs, respectively; L_d,$L_q$are d-axis and q-axis inductances, respectively. By using reference frame transformation, the voltage and torque equations can be also derived in the stator flux reference frame as:

$$v_x = R_s i_x + \frac{d\lambda_x}{dt} = R_s i_x + \frac{d\lambda_s}{dt} \quad (4)$$

$$v_y = R_s i_y + \omega_e \lambda_x = \frac{2R_s}{3p|\lambda_s|} T_e + \omega_e \lambda_s \quad (5)$$

978-1-7281-7296-5/20/$31.00 ©2020 IEEE

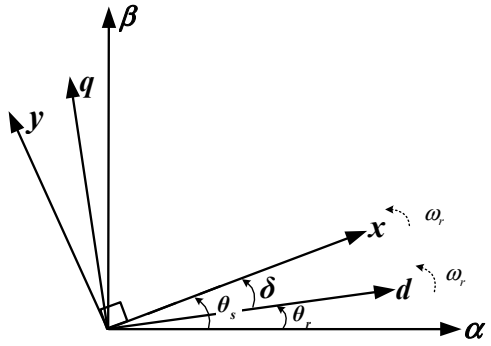

Fig. 1. Vector diagram of IPMSM: (□□) stationary reference frame, (dq) rotor reference frame and (xy) stator flux reference frame.

$$T_e = \frac{3p}{2}|\lambda_s| i_y \tag{6}$$

From (4), the control of flux is obtained by x-axis voltage. Besides, from (5), by using feedforward, the electromagnetic torque is controlled by regulating y-axis voltage.

B. Torque and flux estimator

As torque and flux are typically controlled in DTFC schemes, flux and torque must be estimated. The electromagnetic torque and stator flux can be estimated in the $\alpha\beta$ reference frame as follows:

$$\lambda_\alpha = \int (v_a - R_s i_\alpha)\, dt \tag{7}$$

$$\lambda_\beta = \int (v_\beta - R_s i_\beta) dt \tag{8}$$

$$\lambda_s = \sqrt{\lambda_\alpha^2 + \lambda_\beta^2} \tag{9}$$

$$T_e = \frac{3p}{2}(\lambda_\alpha i_\beta - \lambda_\beta i_\alpha) \tag{10}$$

where $v_{\alpha\beta}$ and $i_{\alpha\beta}$ are the armature voltage and current of motor in the stationary reference frame. Furthermore, as depicted in Fig. 1, θ_s is determined as (11) to transform voltage in the stator flux reference frame to stationary frame for space vector modulation:

$$\theta_s = \tan^{-1}\left(\frac{\lambda_\beta}{\lambda_\alpha}\right) \tag{11}$$

C. Voltage and Current Limitation to Operate Above Base Speed

Above the base speed, motor voltage reaches its maximum so that it should be limited in order to operate in FW region. Maximum voltage of motor is determined as follows:

$$v_d^2 + v_q^2 \le v_{max}^2 = KV_{dc} \tag{12}$$

where K depends on modulation index which is variable based on modulation method. Since space vector modulation is employed in this paper, K is equal to $\sqrt{3}$. Also, (12) is a ellipse in id-iq plane which will shrink with increasing speed. In addition to voltage, current is restricted by inverter or motor current by (13):

$$i_d^2 + i_q^2 \le I_{max}^2 \tag{13}$$

where I_{max} is the maximum current of the motor and equation (13) is also a circle in d-q current plane.

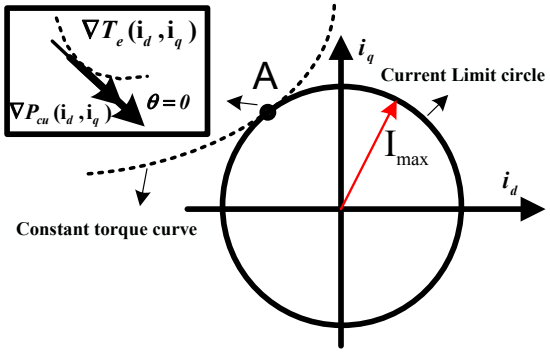

Fig. 2. Constant torque curve, copper losses circle in the id-iq plane.

D. The MTPA strategy for under base speed

In this section, MTPA strategy is employed in order to generate corresponding flux of maximum torque. As depicted in Fig. 2, the A is the point that copper loss and torque curves are tangent. According to Lagrange's theorem, the point A guarantees the minimization of copper loss for the given torque [14,15]. The copper loss of IPMSM can be expressed in terms of d-q current as:

$$P_{cu} = \frac{3}{2} R_s (i_d^2 + i_q^2) \tag{14}$$

By applying the gradient approach and using (3) and (14), MTPA equation is derived as:

$$y = \frac{\partial T_e}{\partial i_d} \times \frac{\partial P_{cu}}{\partial i_q} - \frac{\partial T_e}{\partial i_q} \times \frac{\partial P_{cu}}{\partial i_d} = 0 \tag{15}$$

By substituting and calculating on (15), we have:

$$(L_d - L_q) i_q^2 - \lambda_m i_d - (L_d - L_q) i_d^2 = 0 \tag{16}$$

By realization (16), the flux of MTPA is produced. It should be noted that as far as machine operates below rated speed, MTPA is utilized and therefore flux is constant. Also, maximum torque of machine in any state of operation can be calculated as:

$$T_{limitation} = \frac{3p}{2}|\lambda_s| \sqrt{I_{max}^2 - i_x^2} \tag{17}$$

where i_x and $|\lambda_s|$ are x component of stator current in the stator reference frame and flux magnitude, respectively.

E. The FW strategy for above base speed

As motor reaches base speed, the voltage of motor becomes maximum and so voltage is not able to be controlled. Therefore, flux should reduce in order to control the motor in FW region.

$$\lambda_s = \frac{V_{max}}{\omega_e} = \frac{KV_{dc} - R_s I_{max}}{\omega_e} \tag{18}$$

In addition to the flux reduction, maximum torque starts to reduce as (17) in FW region.

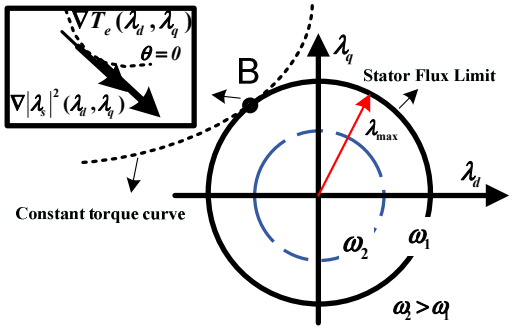

Fig. 3. Constant torque curve, stator flux limit circle in the $\lambda_d - \lambda_q$ plane.

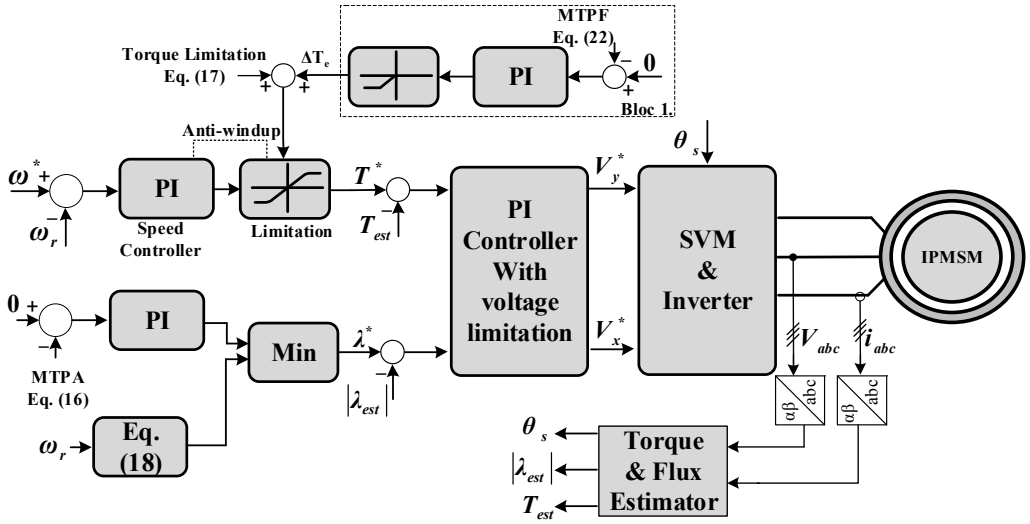

Fig. 4. Proposed control based on DTFC scheme.

III. PROPOSED MTPF STRATEGY FOR ABOVE CRITICAL SPEED

In order to increase speed above the critical speed, MTPF strategy should be used. Furthermore, output power of machine starts to decrease. Indeed, MTPF maximize the ratio of torque to flux. Hence, the stator flux limit equals to:

$$\lambda_d^2 + \lambda_q^2 \le \lambda_{max}^2 = \frac{V_{max}^2}{\omega_e^2} \tag{19}$$

By substituting $i_d = \frac{\lambda_d - \lambda_m}{L_d}$, $i_q = \frac{\lambda_q}{L_q}$ into the (3), the electromagnetic torque is derived in terms of λ_d and λ_q:

$$T_e = \frac{3p}{2} \times \frac{\lambda_q}{L_d L_q}\left(\lambda_m L_q + \left(L_d - L_q\right)\lambda_d\right) \tag{20}$$

Equation (19) represents circle in $\lambda_d - \lambda_q$ plane which will shrink with increasing speed. The tangent of torque curve and the flux limit is demonstrated in Fig. 3 at point B. Based on Lagrange's theorem, the maximum torque is achieved for a given flux above critical speed. According to gradient approach and using (20) and $\lambda_s^2 = \lambda_d^2 + \lambda_q^2$, MTPF equation is given as:

$$z = \frac{\partial T_e}{\partial \lambda_d} \times \frac{\partial |\lambda_s|^2}{\partial \lambda_q} - \frac{\partial T_e}{\partial \lambda_q} \times \frac{\partial |\lambda_s|^2}{\partial \lambda_d} \tag{21}$$

By replacing and doing simplification, (22) is expressed as MTPF:

$$\lambda_q^2\left(L_d - L_q\right) - \lambda_d^2\left(L_d - L_q\right) - \lambda_d \lambda_m L_q = 0 \tag{22}$$

As (22) is regulated by PI, torque limitation equals to:

$$(T_{limitation})_{MTPF} = T_{limitation} + \Delta T_e \tag{23}$$

where ΔT_e is the output of the PI controller. Until motor operates below critical speed, ΔT_e is zero because of using negative saturation. However, ΔT_e is a negative value beyond the critical sped which is variable with increasing speed. It is important to be noted that MTPF is only implemented in the motor whose characteristic current (λ_m / L_d) is inside the current limit circle.

IV. PROPOSED CONTROL SCHEME

The overall block diagram of the proposed scheme is illustrated in Fig. 4. The proposed scheme can operate continuously in both mode of operating without using LUT. In contrast to conventional DTFC, switching frequency of DTFC-SVM is constant. Hence, torque ripple is insignificant in comparison to conventional DTFC in wide speed range. The x-y voltages are produced by flux and torque controller, respectively. According to proposed method which has been discussed in previous section, stator flux of MTPA (16) and FW (18) strategies are generated and being selected their minimum. As shown in Fig. 4, the reference torque, which is generated by the PI speed controller, is limited by anti-windup structure. Under base speed, the limitation of torque is in its maximum value and reference flux is constant. For above base speed, FW flux is chosen so that flux starts to decrease. In this regard, torque limitation also starts to decrease. Above critical speed, the MTPF bloc is activated so that limitation of torque decreases further. It is worth mentioning that saturation of MTPF bloc is $-T_{max}$. Besides, the proposed scheme can operate in all four quadrants with maximum torque of motor. Furthermore, it is able to switch automatically between two regions and works analytically.

V. SIMULATION RESULTS

The simulation is done in order to evaluate the proposed scheme and novel approach of MTPF. The parameter of tested motor is given in Table 1. As it is seen, the λ_m / L_d is inside the current limit circle so that MTPF strategy can be implemented in this motor. The proposed control scheme is simulated in PLECS environment. The simulation results are demonstrated in Figs 5-13. The section one of the simulation investigates the performance of proposed control scheme under base speed from Fig. 5 to Fig. 7. Fig. 7 demonstrates the variation of MTPA bloc variables. Fig. 8 to Fig. 13 shows the next simulation which is the acceleration of IPMSM from 0 to 5000rpm under the load of 0.1 N.m. As shown in Fig .8 and 9, motor can track the speed reference while maximum achievable torque is also obtained in the wide speed range. Below base speed, bloc 1 is disable because of negative saturation and torque is in its maximum value. Once motor crosses the base speed, the torque limitation starts to decrease. However, bloc 1 is still inactive until critical speed which is 3200 rpm. In addition to torque, flux decreases in this time as shown in Fig. 10. As motor crosses the critical speed, bloc 1 is enable automatically and generate negative torque. Furthermore, the torque speed characteristic is shown in Fig. 11. It proves that the proposed scheme can switch from CT,

FW and MTPF smoothly. Also, magnitude of voltages is demonstrated in Fig. 12. In the FW and MTPF regions, the maximum voltage utilization of dc-link is achieved according to Fig. 12. Besides, zero input, feedback that is MTPF equation and the output of bloc 1 is depicted in Fig. 13. It is important to be noted that operating point returns to MTPA strategy as motor reaches the reference speed.

Table 1. The parameter of simulated IPMSM.

Parameters	Value (Unit)
Stator phase resistance (R_s)	18.6 (Ω)
Number of pole pairs	2
Magnet flux linkage	0.18 (Wb)
d-axis inductance (L_d)	0.238 H
q-axis inductance (L_q)	0.5128 H
Moment of inertia	0.00117 Kg.m^2
Friction Coefficient	0.00029 Nm/rad/s
Rated speed	1500 (rpm)
Rated current of inverter	1.28 (A)
Maximum phase voltage	178 (V)
Switching frequency	20 (kHz)
DC link voltage	310 (V)
Maximum Torque	1.2 (N.m)

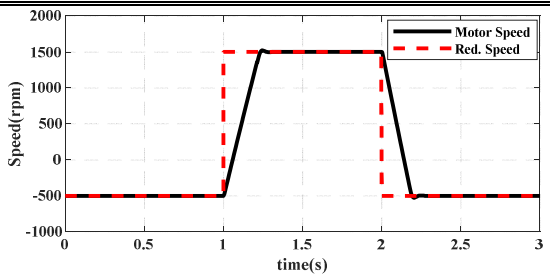

Fig. 5. The performance of motor speed under the rated speed

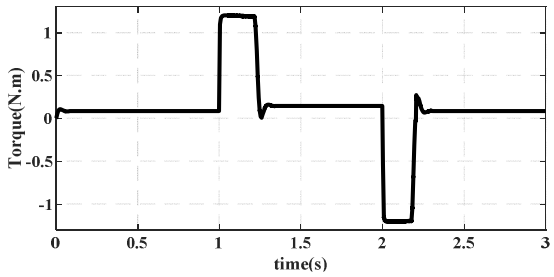

Fig. 6. The simulation result of torque under the base speed

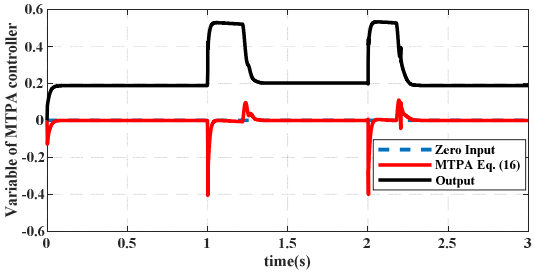

Fig. 7. The variation of MTPA controller variables

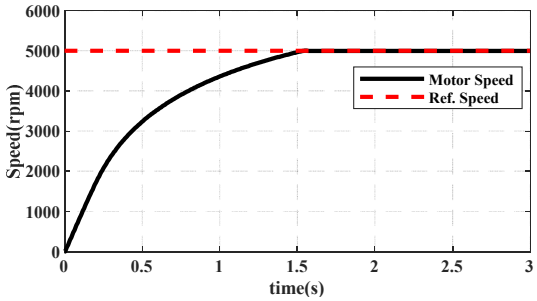

Fig. 8. The simulation result of speed response for the acceleration from 0 to 5000rpm

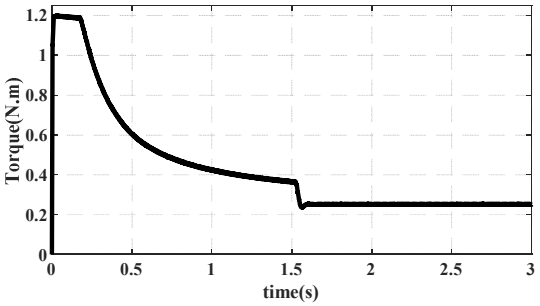

Fig. 9. The simulation result of torque characteristic

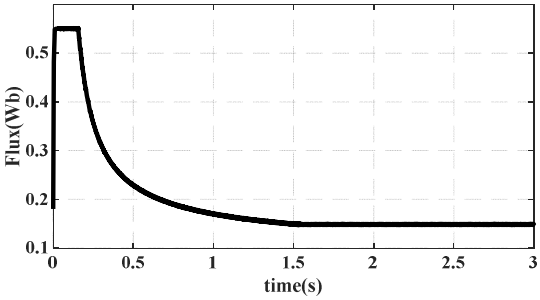

Fig. 10. The variation of flux during acceleration

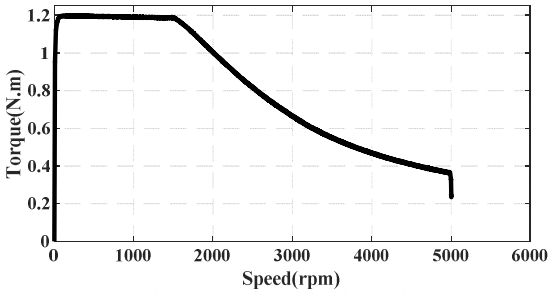

Fig. 11. Torque-speed characteristic under the 0.1 load torque

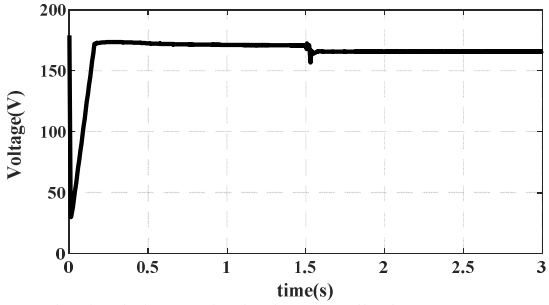

Fig. 12. The simulation result of voltage amplitude

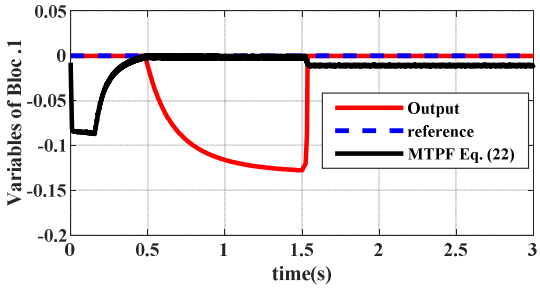

Fig. 13. Variation of bloc .1 variables during acceleration

VI. CONCLUSION

A novel method to generate required torque to track MTPF has been investigated in this paper. Indeed, the torque to flux ratio is maximized based on Lagrange's theorem in order to operate above critical speed. Then, the MTPF expression was obtained by gradient method. Moreover, the control method is based on DTFC and pre-experimental result is not needed to generate corresponding flux. The proposed scheme can control motor automatically above critical speed. It is suggested to consider saturation in the experimental test, which is the future scope, to increase the accuracy. The simulation was realized to prove the stability behavior of the proposed control scheme.

REFERENCES

[1] A. Emadi, *Advanced Electric Drive Vehicles*. CRC Press, 2014.

[2] R. Krishnan, *Permanent Magnet Synchronous and Brushless DC Motor Drives*. 2010.

[3] M. F. Rahman, L. Zhong, and Khiang Wee Lim, "A direct torque-controlled interior permanent magnet synchronous motor drive incorporating field weakening," *IEEE Trans. Ind. Appl.*, vol. 34, no. 6, pp. 1246–1253, 1998.

[4] F. Niu, B. Wang, A. S. Babel, K. Li, and E. G. Strangas, "Comparative Evaluation of Direct Torque Control Strategies for Permanent Magnet Synchronous Machines," *IEEE Trans. Power Electron.*, vol. 31, no. 2, pp. 1408–1424, Feb. 2016.

[5] G. Foo, C. S. Goon, and M. F. Rahman, "Analysis and Design of the SVM Direct Torque and Flux Controlled IPM Synchronous Motor Drive," *Aust. J. Electr. Electron. Eng.*, vol. 7, no. 1, pp. 21–30, Jan. 2010.

[6] L. Tang, L. Zhong, M. F. Rahman, and Y. Hu, "A Novel Direct Torque Controlled Interior Permanent Magnet Synchronous Machine Drive With Low Ripple in Flux and Torque and Fixed Switching Frequency," *IEEE Trans. Power Electron.*, vol. 19, no. 2, pp. 346–354, Mar. 2004.

[7] S. Ekanayake, R. Dutta, M. F. Rahman, and D. Xiao, "Direct torque and flux control of interior permanent magnet synchronous machine in deep flux-weakening region," *IET Electr. Power Appl.*, vol. 12, no. 1, pp. 98–105, Jan. 2018.

[8] Y. Chen *et al.*, "Improved Flux-Weakening Control of IPMSMs Based on Torque Feedforward Technique," *IEEE Trans. Power Electron.*, vol. 33, no. 12, pp. 10970–10978, Dec. 2018.

[9] G. Pellegrino, E. Armando, and P. Guglielmi, "Direct-Flux Vector Control of IPM Motor Drives in the Maximum Torque Per Voltage Speed Range," *IEEE Trans. Ind. Electron.*, vol. 59, no. 10, pp. 3780–3788, Oct. 2012.

[10] S. M. Showvbul Islam Shakib *et al.*, "An Analytical Approach to Direct Torque and Flux Control of Interior Permanent Magnet Synchronous Machine for Deep Field Weakening Without Using Pre-calculated Lookup Tables," *ICPE 2019 - ECCE Asia - 10th Int. Conf. Power Electron. - ECCE Asia*, vol. 3, pp. 3196–3202, 2019.

[11] S. A. Atashin, H. A. Zarchi, and G. R. A. Markadeh, "Maximum Torque of IPMSM in Wide Speed Range Based on Current Angle Approach," *2020 11th International Power Electronics, Drive Systems and Technologies Conference (PEDSTC), Tehran, Iran,2020, pp. 1-1*.

[12] J. Faiz and S. H. Mohseni-Zonoozi, "A novel technique for estimation and control of stator flux of a salient-pole PMSM in DTC method based on MTPF," *IEEE Trans. Ind. Electron.*, vol. 50, no. 2, pp. 262–271, Apr. 2003.

[13] A. Shinohara, Y. Inoue, S. Morimoto, and M. Sanada, "Asymptotic MTPF control for high-speed operations in direct torque controlled IPMSM drives," in *2017 IEEE 12th International Conference on Power Electronics and Drive Systems (PEDS)*, 2017, vol. 2017-Decem, no. December, pp. 816–821.

[14] H. Abootorabi Zarchi, H. Mosaddegh Hesar, and M. Ayaz Khoshhava, "Online maximum torque per power losses strategy for indirect rotor flux-oriented control-based induction motor drives," *IET Electr. Power Appl.*, vol. 13, no. 2, pp. 259–265, Feb. 2019.

[15] M.-A. Salahmanesh, H. A. Zarchi, and H. M. Hesar, "Lyapunov - Based Input-Output Feedback Linearization Control of Induction Motor drives Considering Online MTPA Strategy and Iron Loss," in *2019 27th Iranian Conference on Electrical Engineering (ICEE)*, 2019, pp. 697–701.